Direct evaluation of composition profile, strain relaxation, and elastic energy of Ge:Si(001) self-assembled islands by anomalous x-ray scattering

R. Magalhães-Paniago,[1,2] G. Medeiros-Ribeiro,[2,3] A. Malachias,[1] S. Kycia,[2] T. I. Kamins,[3] and R. Stan Williams[3]
[1]*Departamento de Física, Universidade Federal de Minas Gerais, MG, Brazil*
[2]*Laboratório Nacional de Luz Síncrotron, Campinas, Brazil*
[3]*Hewlett-Packard Laboratories, 1501 Page Mill Rd., Palo Alto, California 94117*
(Received 9 August 2002; published 19 December 2002)

The growth of strained epitaxial self assembled nanocrystals is comprised of a variety of kinetic and thermodynamic factors that determine their morphology and size. Some of the significant factors to their stability are strain and interdiffusion. Here we directly measure the gradient of composition and strain in Ge nanocrystals grown on Si(001) using anomalous x-ray scattering. By combining our x-ray results, where we relate strain, interdiffusion, and shape with atomic force microscopy measurements, we have been able to determine the complete strain configuration of these islands. We show that the amount of elastic energy in pyramids and domes can be evaluated. The transition from pyramids to domes is accompanied by an increase of lattice parameter and enhancement of interdiffusion, both leading to a drastic decrease of the elastic energy stored per atom.

DOI: 10.1103/PhysRevB.66.245312 PACS number(s): 68.65.−k

I. INTRODUCTION

There has been a considerable debate regarding the growth mechanisms of self-assembled islands in heteroepitaxial growth of lattice mismatched systems. Most importantly, the stability of nanocrystal size and shape is important should one desire to control the electronic properties of such systems in a systematic way. Basically, the growth of nanocrystals may proceed via Ostwald ripening processes where no stable size[1] or shape exist,[2] or they can represent a local minimum and therefore correspond to a metastable structure.[3–5] In the first scenario islands can grow with no restriction, and moreover, the size distribution worsens with time. Experimental evidences favoring Ostwald ripening exist in the work of Ross *et al.*,[2] where real time growth movies of Ge on Si (001) were performed and the continuing growth of island size persisted during the experiment. Coarsening nevertheless has been observed in situations where interdiffusion is severe.[6] Favoring the thermodynamic stability of nanocrystals, experiments performed in a variety of Ge:Si samples provided statistically significant results that fail in verifying the ripening models.[7] More recently,[8] simulations have shown alternate possibilities for island ensemble stability against coarsening.

Strain and interdiffusion are key parameters that influence island growth and therefore essential in discerning the issues of coarsening and stability. Earlier x-ray studies of Ge:Si (001) grown at high temperatures and under annealing[9] qualitatively revealed the change in island lattice parameter. Later on[10] the composition profile indicating the presence of Si in Ge:Si (001) islands was confirmed via scanning transmission electron microscopy and energy-dispersive x-ray analysis, as well as x-ray-absorption fine structure[11] and x-ray photoelectron spectroscopy.[12] Electron microscopy studies[13,14] and modeling revealed the average strain of Ge:Si (001) islands, and their composition was also consistent with previous results. High intensity x-ray experiments performed with synchrotron sources in grazing incidence geometry (GIXRD) started earlier on,[15] revealing the lattice parameter distribution of Ge:Si hut clusters. Also for InAs:GaAs (001) surface islands[16] the strain and composition profile was extracted by GIXRD experiments utilizing a scattering model. However, no elastic energy data was evaluated and the method can only be applied to III-V compounds. Therefore a general tool for the study of the strain-composition interplay during growth and the evaluation of elastic energy of heteroepitaxial self assembled dots is still lacking.

In this paper, we simultaneously profile the lattice parameter and composition by a single probe, anomalous x-ray scattering. Combining these data with atomic force microscopy (AFM) allowed us to directly evaluate and compare the elastic energy stored in Ge pyramids and domes. We show that the transition from one shape to the other is accompanied by a decrease of the elastic energy per atom of these islands, induced both by an increase in lattice parameter as well as in interdiffusion. These quantitative results are consistent with the assumption that higher aspect ratio islands store less elastic energy.

II. EXPERIMENT

Germanium was grown by chemical vapor deposition on Si(001) substrates; the growth details are described in Ref. 7. For sample A (pyramids), 5.9 monolayers (ML) of Ge were deposited at 0.1 ML/s, for a total deposition time of 60 s whereas for sample B (domes), 11.2 ML were deposited at 0.05 ML/s for a total deposition time of 240 s. Although the growth rates were different, 0.1 ML/s represents the upper limit for low supersaturation conditions for the growth of Ge at 600 °C.

Figure 1 summarizes the main characteristics of both systems studied, as obtained by AFM statistics. (a) and (b) show 100×100-nm AFM scans on samples A and B, respectively, along with their corresponding line scans. The grayscale in

 ©2002 The American Physical Society

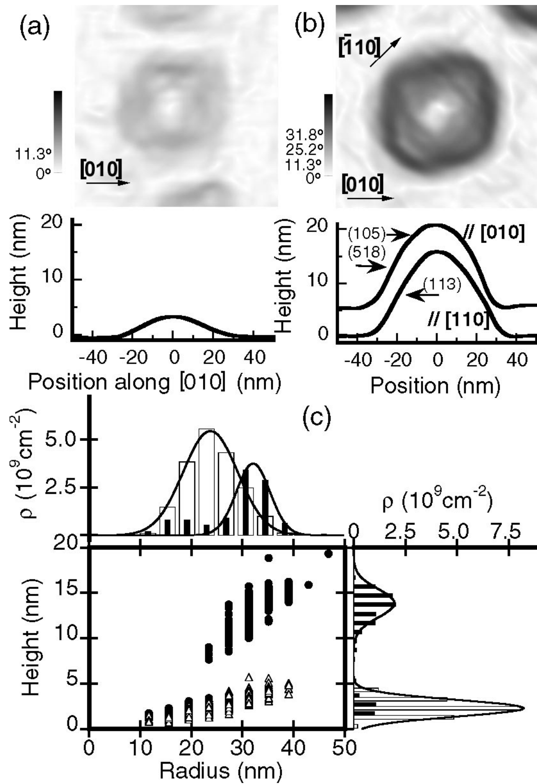

FIG. 1. AFM experiments and analysis performed on samples A (pyramids) and B (domes). (a) top image: 100×100-nm AFM scan of a typical pyramid on sample A, displayed as the local slope with respect to the substrate, with the corresponding scale. The grayscale is keyed to the angle between the normal at each point and the growth direction [001]; bottom: line scan taken along the [010] direction; the facets are (105). (b) top image: 100×100-nm AFM scan of a typical dome on sample B, with the same grayscale convention; bottom: line scans taken along [010] and [110] directions. (c) Upper: island density as a function of radius. Lower: radius vs height size distribution for both pyramids (triangles) and domes (circles). The lines are fitted Gaussian functions that yielded the size distributions given in the text.

the AFM images is keyed to the angle between the normal and the growth direction, white corresponding to flat areas and dark to steep facets. The facets that these islands contain are indicated in the line scans as well as by the shades of gray in the AFM scan. The two island shapes portrayed in the AFM scans, pyramid and dome, are representatives of the measured ensembles. Figure 1(c) shows the statistical analysis performed in 4-μm^2 areas on samples A (empty symbols and bars) and B (filled symbols and bars). The first observation is that the ensembles are monodisperse for both samples comprised of islands of different shapes, with pyramids of height 3.0 ± 1.0 nm and radius 23.9 ± 6.5 nm and domes of height 14.2 ± 1.9 nm and radius 32.3 ± 4.0 nm.

The x-ray scattering experiments were performed at the beamline XD2 at the Brazilian National Synchrotron Light Source. This beamline is equipped with a double-crystal Si(111) monochromator with the second crystal being sagitally focused to the center of a standard four-circle Huber diffractometer. The in-plane structure of the islands was determined by grazing incidence angular and radial x-ray scans performed near the (220) Si reflection, all done at an incident angle of 0.35°, where the scattering was collected integrating the exit angle from 0° up to 1.5°. The relationship between the lattice parameter and local radius of the islands was inferred from angular scans at a fixed radial position $[q_r=(4\pi/\lambda)\sin(2\theta/2)]$ [Figs. 2(a) and (b)].[16] Angular scans correspond to measurements where the scattering angle 2θ is kept constant and the angle θ between the x-ray beam and the Bragg planes perpendicular to the sample surface is varied. This measurement essentially probes regions of the crystal with a specific lattice parameter d given by Bragg's law $\lambda=2d(\sin 2\theta/2)$. In momentum transfer space, only the angular momentum transfer $q_a=(4\pi/\lambda)\sin(\theta-2\theta/2)$ is varied, while the radial momentum transfer q_r is kept constant. In this case the scattering profile is essentially the square of the Fourier transform of the shape function of a section of the island with a specific lattice parameter $a'=d^*(h^2+k^2+l^2)^{1/2}$, where h, k, and l are the indices of the reflection.

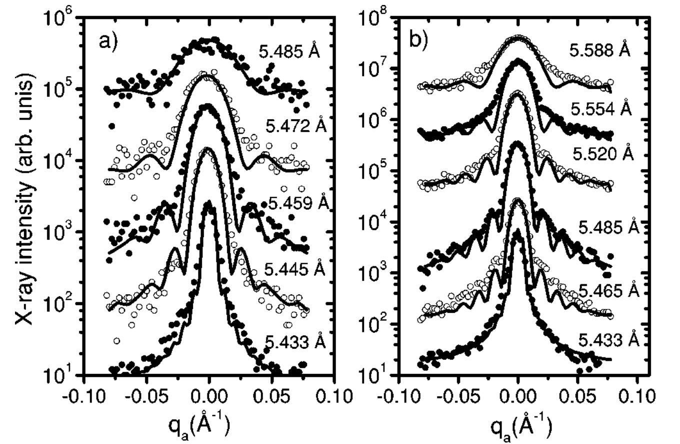

FIG. 2. (a) Angular x-ray scans along the [1-10] direction of pyramids for selected lattice parameters a', together with least-squares fits (see text). The fits included the size distribution obtained from the AFM data. (b) Same measurements for domes, with a broader range of lattice parameter a'.

For the determination of the Si/Ge interdiffusion inside the islands, anomalous x-ray radial scans well below ($E=11\,000$ eV) and at the Ge K absorption edge (11 103 eV) were performed. These radial scans correspond to conventional θ-2θ scans, where the fraction of the islands with a specific lattice parameter a' contribute to the scattering at a specific 2θ position, also given by Bragg's law. The comparison between the scattered intensity at the same value of q_r for two different energies near the Ge edge allows us to infer the Ge concentration as a function of lattice parameter $a'=(2\pi/q_r)(h^2+k^2+l^2)^{1/2}$.

III. RESULTS AND ANALYSIS

In Fig. 2 we show angular x-ray scans along the [1–10] direction of pyramids for selected lattice parameters a'. Least-square fits were performed assuming that the islands have a square section of side L, i.e., $I(q_a)\propto|\sin(q_aL/2)/q_a|^2$, with L as a fitting parameter. From these

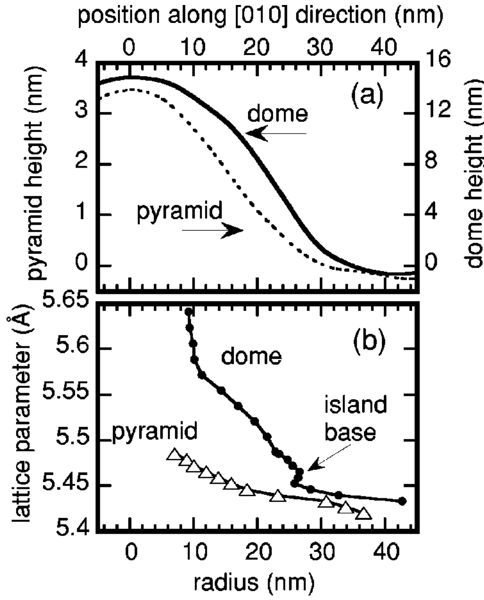

FIG. 3. (a) AFM line scans on a most statistically significant pyramid (left axis, dashed line) and dome (right axis, solid line). (b) Radius versus lattice parameter, obtained from Fig. 2; filled circles correspond to domes and open triangles to pyramids.

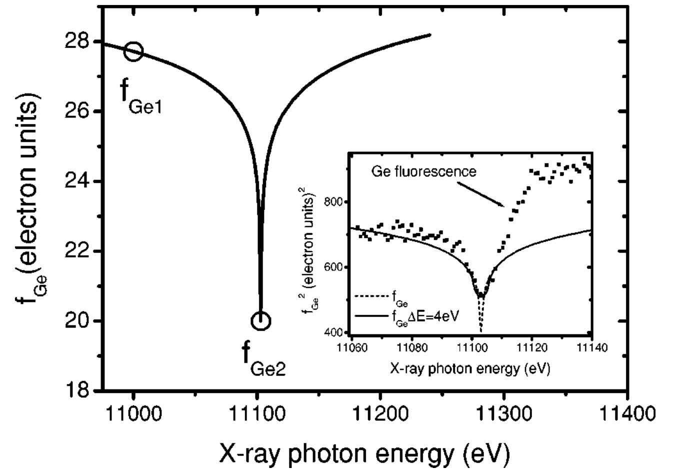

FIG. 4. Variation of the real part of the atomic scattering factor of germanium as a function of photon energy near its *K*-edge. Notice the drastic decrease of $f_{\rm Ge}$ at 11 103.1 eV. The two energies used in this experiment are indicated by circles ($f_{\rm Ge1}$ and $f_{\rm Ge2}$). Inset: comparison of the square of the Ge scattering factor (dashed line) and its value averaged over an energy window of 4 eV (solid line) with the x-ray scattered intensity from Ge islands. Notice the Ge fluorescence present above the *K*-edge. The use of this energy window allows us to work right at the absorption edge, since the average scattering factor remains constant for an energy fluctuation of 3 eV (much larger than the fluctuation of 0.5 eV of our experimental setup).

data a relationship between the local lattice parameter a' and the outer diameter L for several regions of pyramids and domes was obtained. The fits included the size distribution obtained from the AFM data as well as the experimental resolution of the diffractometer, which broadens out the intensity maxima usually observed in these fits. By correlating these data [Figs. 2(a) and (b)] with the AFM line scans (which gives us the relationship between diameter L and height, see Figs. 1(a) and (b), we obtained the variation of the lattice parameter as a function of height.

Figures 3(a) and (b) show the pyramid and dome AFM line profiles and their lattice parameter to radius relation [inferred from Figs. 2(a) and (b)]. For the pyramids (empty triangles—sample A) this relationship is monotonic, indicating a smaller lattice parameter for increasing radii. As for the domes (filled circles—sample B), a more complex dependence is revealed and, most importantly, the fact that it is no longer monotonic. The reason for the decrease in radius for decreasing lattice parameters around 5.46 Å is that we have reached the island base. Therefore it means that we are probing regions of constant lattice parameter *under* the island, which have smaller radii than the island base. Therefore by a comparison between the x-ray results and the AFM profile it is clearly possible to determine the strain created by the domes in the substrate. These results are consistent with finite element as well as molecular-dynamics calculations using elasticity theory,[17] which proved that there is a sizeable strain effect from a Ge nanocrystal on the underlying region of the substrate. It must be noted that the lateral sizes obtained by AFM represent an upper limit for the lateral sizes determined by x-ray experiments for two reasons, namely: (i) surface native oxide that does not scatter the x-ray photons but it is measured by AFM, and (ii) tip convolution effects. Nevertheless, this effect can be accounted for, and the comparisons hereafter between AFM and x-ray data have been properly adjusted.

In order to determine the local content of Ge in both types of nanocrystals we measured the change in scattering intensity [as a function of q_r, meaning as a function of lattice parameter $a' = (2\pi/q_r)(h^2+k^2+l^2)^{1/2}$] for two specific energies near the Ge K absorption edge. As shown in Fig. 4, by tuning the x-ray energy near the Ge *K*-edge, the Ge atomic scattering factor $f_{\rm Ge}$ diminishes by 28.6%. Since the islands are composed of two species, the x-ray scattered intensity is proportional to the square of the sum of the concentration of each one multiplied by the corresponding (Ge or Si) scattering factor $I_{hkl} = A[C_{\rm Ge}f_{\rm Ge} + C_{\rm Si}f_{\rm Si}]^2$ where $C_{\rm Ge}+C_{\rm Si}=1$ and A is a constant. From the ratio of the scattered intensity for two different x-ray energies

$$\frac{I_1}{I_2} = \left(\frac{C_{\rm Ge}f_{\rm Ge1} + C_{\rm Si}f_{\rm Si}}{C_{\rm Ge}f_{\rm Ge2} + C_{\rm Si}f_{\rm Si}}\right)^2, \tag{1}$$

where I_1 and I_2 are the measured x-ray intensities and $f_{\rm Ge1}$ and $f_{\rm Ge2}$ the Ge scattering factors at 11 000 and 11 103 eV, respectively, the Ge concentration was determined from

$$C_{\rm Ge} = \left(1 + \frac{f_{\rm Ge2}\sqrt{I_1} - f_{\rm Ge1}\sqrt{I_2}}{f_{\rm Si}(\sqrt{I_2} - \sqrt{I_1})}\right)^{-1}. \tag{2}$$

Since the Ge scattering factor varies rapidly near its *K*-edge, the x-ray beam was set with a broad energy width of 4 eV to minimize possible energy fluctuations and to make this variation smoother (systematic checks on the stability of the x-ray monochromator over runs of 8 h, during the 6 days of the

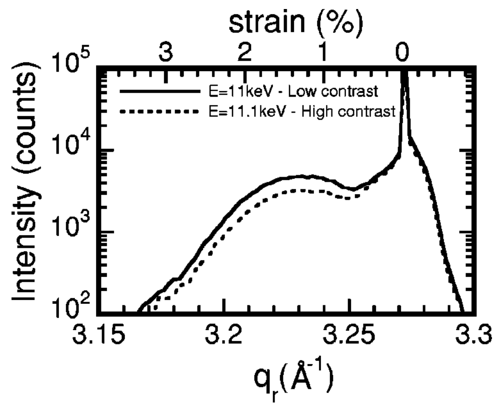

FIG. 5. Anomalous x-ray radial scans carried out on domes. The difference in scattering in the two curves comes from the presence of Ge atoms inside the islands. Therefore, for lattice parameters closer to the island base, a higher percentage of Si can be inferred, as it can be readily seen on the asymptotic behavior of the two curves towards the Si lattice parameter. The strain axis indicates the difference in lattice parameter with respect to the value for silicon.

experiment, showed that the energy fluctuations of the x-ray monochromator were smaller than 0.5 eV). The tuning of the photon energy width was obtained by varying the beam size both before and after the monochromator with vertical slits. The calibration of the x-ray photon energy was first performed by measuring both the fluorescence yield as well as the absorption spectrum of a Ge absorber near the Ge *K*-edge, varying the incident photon energy from 10 800 eV up to 11 200 eV. Finally, the minimum of the Ge scattering factor at the *K*-edge was confirmed by measuring the x-ray scattering signal from the Ge islands near the Si 220 reflection (see the inset of Fig. 4), a procedure similar to the one performed by Specht and Walker.[18] For the results presented below the Ge scattering factors were calculated averaging over the energy window of 4 eV and standard atomic scattering factors tables were used.[19]

In Fig. 5 we show radial scans for the dome samples, where the change in the scattering intensity for two x-ray energies near the Ge edge is clearly observed. The Si (2 2 0) substrate peak is clearly seen, and the island signal occurs at larger in-plane lattice parameters, meaning lower momentum transfer. The difference in intensity varies from 0 to 30% for this particular case depending on the strain state of the islands (considering the scattering factors for these two specific x-ray energies and the energy resolution of 4 eV, for pure Ge it would change by 35%). This basically states that there is a substantial amount of Si inside the domes, most notably at the island base. By performing this procedure for selected lattice parameters (meaning selected 2θ angles) we have extracted the dependence of the Ge concentration C_{Ge} to the lateral lattice parameter a' and mapped out the compositional profile for the two types of islands.

Figure 6 shows the Ge content as a function of lattice parameter, inferred from Fig. 5 and a similar measurement on pyramids (not shown here). It can be seen that the average Ge content on pyramids is much higher than on domes. Also, the lattice relaxation is larger for domes than for pyramids. From the combination of the results of Figs. 3 and 6, we

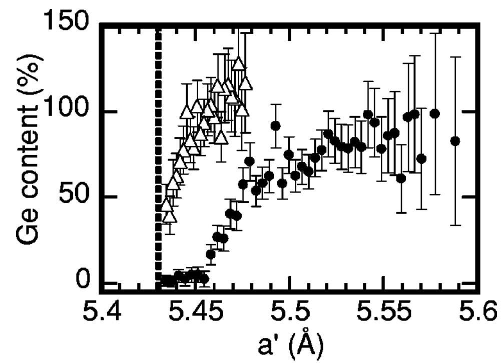

FIG. 6. Ge content in pyramids and domes as a function of the in-plane lattice parameter a'. The error bars were calculated taking into account the statistical fluctuations of the data of Fig. 5 as well as the uncertainties in f_{Ge1} and f_{Ge2} for a 0.5-eV fluctuation of the x-ray energy. Note that the uncertainties increase for decreasing x-ray signal intensities, which depend on the amount of scattering material.

obtained the variation of the Ge concentration as a function of height. As mentioned earlier, the radii inferred from X-ray experiments had to be corrected in order to include the effects of surface oxide if we wish to map the composition, lattice parameter and strain as a function of height. The correction consisted of adding 2 nm to the radii inferred from the x-ray data (2 nm was the value obtained by comparison at the island base, and it is in accord with what is considered as typical native oxide thickness). Figure 7 displays the dependence of the Ge composition on the island height. For the case of pyramids, it is clear that there is very little interdiffusion, which occurs only at the island-substrate interface. As for the domes, a substantial amount of Si interdiffusion takes place throughout the island, reaching 40% at half the island height. From all these experimental results, it can be anticipated that on a per-atom basis pyramids store more elastic energy than domes. Before evaluating stored energies, further analysis can improve our understanding on the strain status of these islands.

One cannot determine strain without a simultaneous measurement of both local lattice parameter and composition of the nanocrystal. This is because the change in lattice param-

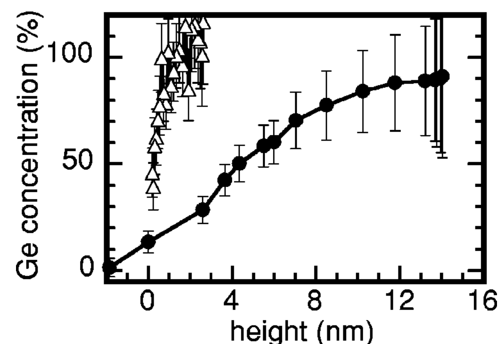

FIG. 7. Ge content as a function of height for (a) pyramids and (b) domes composed with typical atomic force microscopy measurements of both samples. Notice the drastic increase in the Si content in the domes.

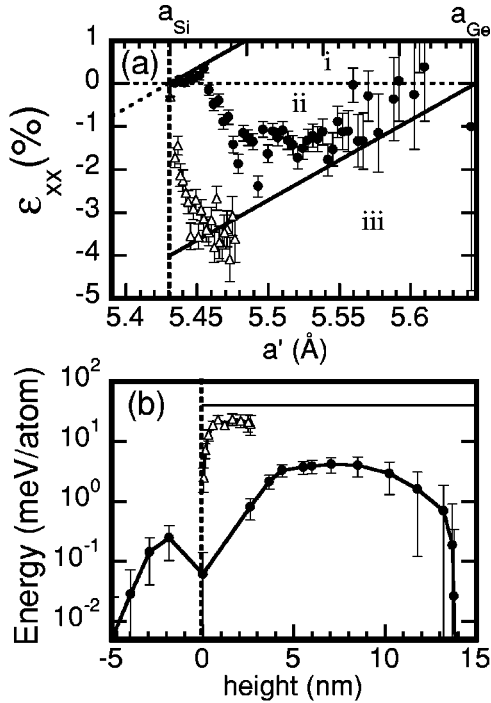

FIG. 8. (a) in-plane strain ε_{xx} as a function of a' for pyramids and domes. Vertical dashed line corresponds to the Si lattice parameter whereas horizontal dashed line corresponds to zero strain condition; i.e., that of a SiGe unstressed alloy. Upper and lower diagonal lines define the strain of a pure Si and Ge layer, respectively, grown on a substrate of lattice parameter a'. Regions i and ii correspond to tensile and compressive strain. Region iii is only accessible by external applied stress (the data points that lie within region iii are accounted for primarily the error bars). Finally, data falling along the Si diagonal dashed line would correspond to compressed Si. (b) Energy on a per atom basis as a function of height for an uniformly strained 2D Ge layer (solid line), pyramids (triangles), and domes (filled circles).

eter can be both due to substrate imposed stress as well as change in composition. The correct value of the local strain of the nanocrystal with local composition Si_xGe_{1-x} is given by $\varepsilon = a'/a(x) - 1$, where $a(x)$ is the lattice parameter of an unstrained alloy [calculated using Vegard's law, $a(x) = x\ a_{\mathrm{Si}} + (1-x)\ a_{\mathrm{Ge}}$] and a' is the local lattice parameter.

Figure 8(a) displays the value of the lateral strain ε_{xx}, determined from the measured in-plane lattice parameter a' (Fig. 3) and the local chemical composition of Fig. 6, as a function of a'. The empty triangles and filled circles again correspond to pyramids (sample A) and domes (sample B). This plot can be divided in three regions: (i) tensile material ($\varepsilon_{xx} > 0$); (ii) compressed material ($\varepsilon_{xx} < 0$); and (iii) externally stressed material (from an external source). The diagonal solid lines correspond to the strain of a pure Ge (lower) or Si (upper) layer grown on a substrate of lattice parameter a'. Outside the region defined by these diagonals and the bounds at a_{Si} and a_{Ge} (vertical dashed lines) no island data can exist, with two exceptions: externally stressed material [region (iii)], and the compressed Si regions in the substrate (along the diagonal dashed line—not accessible in this experiment, but observed under different scattering geometries[20]). One can see then that the average strain in pyramids and domes is about 3% and 1.5%. Moreover, for the domes the underlying tensile stressed substrate (data lying along the Si diagonal line) can be observed.

One can calculate the elastic energy per volume at a position i at the island according to[21]

$$E = 2\mu\left(\frac{1+\nu}{1-\nu}\right)\varepsilon^2 \tag{3}$$

with μ and ν as the shear modulus and poisson ratio of the GeSi alloy, and ε as the local strain, as defined and mapped in Fig. 8(a). From this relation we can extract the elastic energy on a per atom basis by using the SiGe atom density. Figure 8(b) shows the elastic energy height dependence for a two-dimensional (2D) uniformly strained pure Ge film grown on a Si substrate (solid line), for pyramids (empty triangles) and domes (filled domes).

IV. DISCUSSION AND CONCLUSIONS

Several conclusions can be drawn from Fig. 8(b). First, the amount of elastic energy stored per atom in the nanocrystal is considerably larger than underneath it. One must consider, however, that this strained region below the substrate-islands interface is larger than the island bottom area and that the compressed Si region around the island is not included. It is also noticeable that at the island-substrate interface there is a local minimum for the elastic energy. This is due to the change of stress from compressive to tensile, as the chemical composition changes from germanium to silicon. The most important result of Fig. 8(b), however, is that the average energy stored per atom for a two-dimensional layer is roughly twice that of a pyramid and ten times larger than that of a dome. This clearly shows that the shape transition from pyramids to domes observed at the coverage of 6–8 monolayers of Ge leads to a considerable decrease in the volume energy per atom of the nanocrystal.

Perhaps the most intriguing point in our observations is that in a matter of 180 sec a significant amount of Si is already incorporated into the islands. Interdiffusion has been characterized for submonolayer growth of Ge:Si(001),[22] as well as in layers of GeSi alloys.[23] Nevertheless, the processes occurring at these limits for 2D growth are very different when contrasted with 3D growth, and in fact take place in much longer time scales. There are several differences that should change the way intermixing take place: (i) there is no longer biaxial strain, (ii) the surface chemical potential is a function of local strain, and therefore will drive surface diffusion in a much more significant way than interdiffusion that takes place by either exchange of atoms or interstitials, and (iii) the existence of trenches around the domes extending into the substrate,[24] which will act as a Si reservoir. In comparing the pyramid and domes compositional profile, it is plausible that the influence of the trenches is more effective in providing Si into the islands (pyramids do not have trenches) than bulk interdiffusion.

In summary, we have shown that by a direct measurement of both lattice parameter and composition of Ge:Si pyramids

and domes grown on Si(001) the elastic energy could be accurately evaluated. The use of x-ray anomalous scattering as well as the combination of lattice parameter and composition measurements are essential for the correct evaluation of elastic stored energies in Ge nanocrystals. This method can be generally applied to any other heretoepitaxial system. In the Ge:Si(001) case, we observed a considerable decrease in energy from pyramids to domes, which is induced both by the increase of lattice parameter as well as an enhancement in intermixing.

ACKNOWLEDGMENTS

R.M.P. acknowledges the support of CNPq and ABTLuS, and S. C. Moss for a careful reading of the manuscript. G.M.R. thanks FAPESP Contract No. 98/14757-4 and CNPq for financial support, and J. Tersoff for fruitful discussions.

[1] M. Zinke-Allmang, L. C. Feldman, and M. H. Grabow, Surf. Sci. Rep. **16**, 377 (1992).

[2] F. M. Ross, J. Tersoff, and R. M. Tromp, Phys. Rev. Lett. **80**, 984 (1998).

[3] I. Daruka and A.-L. Barabási, Phys. Rev. Lett. **79**, 3708 (1997).

[4] V. A. Shchukin, N. N. Ledentsov, P. S. Kop'ev, and D. Bimberg, Phys. Rev. Lett. **75**, 2968 (1995).

[5] G. Medeiros-Ribeiro, A. M. Bratkovski, T. I. Kamins, D. A. A. Ohlberg, and R. Stanley Williams, Science **279**, 353 (1998).

[6] J. A. Floro, G. A. Lucadamo, E. Chason, L. B. Freund, M. Sinclair, R. D. Twesten, and R. Q. Hwang, Phys. Rev. Lett. **80**, 4717 (1998).

[7] T. I. Kamins, G. Medeiros-Ribeiro, D. A. A. Ohlberg, and R. Stanley Williams, J. Appl. Phys. **85**, 1159 (1999).

[8] Cheng-Hsin Chiu, Appl. Phys. Lett. **75**, 3473 (1999); Y. W. Zhang and A. F. Bower, *ibid.* **78**, 2706 (2001).

[9] T. I. Kamins, G. Medeiros-Ribeiro, D. A. A. Ohlberg, and R. S. Williams, Appl. Phys. A: Mater. Sci. Process. **67**, 1 (1998).

[10] S. A. Chaparro, Jeff Drucker, Y. Zhang, D. Chandrasekhar, M. R. McCartney, and David J. Smith, Phys. Rev. Lett. **83**, 1199 (1999).

[11] F. Boscherini, G. Capellini, L. Di Gaspare, F. Rosei, N. Motta, and S. Mobilio, Appl. Phys. Lett. **76**, 682 (2000).

[12] G. Capellini, M. De Seta, and F. Evangelisti, Appl. Phys. Lett. **78**, 303 (2001).

[13] Peter D. Miller, Chuan-Pu Liu, William L. Henstrom, J. Murray Gibson, Y. Huang, P. Zhang, T. I. Kamins, D. P. Basile, and R. Stanley Williams, Appl. Phys. Lett. **75**, 46 (1999).

[14] Chuan-Pu Liu, J. Murray Gibson, David G. Cahill, Theodore I. Kamins, David P. Basile, and R. Stanley Williams, Phys. Rev. Lett. **84**, 1958 (2000); William L. Henstrom, Chuan-Pu Liu, J. Murray Gibson, T. I. Kamins, and R. Stanley Williams, Appl. Phys. Lett. **77**, 1623 (2000).

[15] A. J. Steinfort, P. M. L. O. Scholte, A. Ettema, F. Tuinstra, M. Nielsen, E. Landemark, D.-M. Smilgies, R. Feidenhans'l, G. Falkenberg, L. Seehofer, and R. L. Johnson, Phys. Rev. Lett. **77**, 2009 (1996).

[16] I. Kegel, T. H. Metzger, A. Lorke, J. Peisl, J. Stangl, G. Bauer, J. M. García, and P. M. Petroff, Phys. Rev. Lett. **85**, 1694 (2000); I. Kegel, T. H. Metzger, A. Lorke, J. Peisl, J. Stangl, G. Bauer, K. Nordlund, W. V. Schoenfeld, and P. M. Petroff, Phys. Rev. B **63**, 035318 (2001).

[17] P. Raiteri, Leo Miglio, F. Valentinotti, and M. Celino, Appl. Phys. Lett. **80**, 3736 (2002).

[18] E. D. Specht and F. J. Walker, Phys. Rev. B **47**, 13 743 (1993).

[19] S. Sasaki, KEK report 88-13, February 1989, Tsukuba-shi, Japan.

[20] Z. M. Jiang, X. M. Jiang, W. R. Jiang, Q. J. Jia, W. L. Zheng, and D. C. Qian, Appl. Phys. Lett. **76**, 3397 (2000).

[21] See, e.g., J. Y. Tsao, *Materials Fundamentals of Molecular Beam Epitaxy* (Academic, San Diego, CA, 1993).

[22] Blas P. Uberuaga, Michael Leskovar, Arthur P. Smith, Hannes Jónsson, and Marjorie Olmstead, Phys. Rev. Lett. **84**, 2441 (2000).

[23] N. R. Zangenberg, J. Lundsgaard Hansen, J. Fage-Pedersen, and A. Nylandsted Larsen, Phys. Rev. Lett. **87**, 125901 (2001).

[24] S. A. Chaparro, Y. Zhang, and Jeff Drucker, Appl. Phys. Lett. **76**, 3534 (2000), Ulrich Denker, Oliver G. Schmidt, Neng-Yun Jin-Philipp, and Karl Eberl, *ibid.* **78**, 3723 (2001).